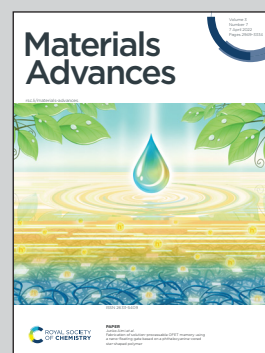Showcasing research from Dr Shoji Nagaoka's laboratory, Materials Development Department, Kumamoto Industrial Research Institute, Kumamoto, Japan.

Co-assembling system that exhibits bright circularly polarized luminescence

We demonstrate that a co-assembling system comprising a nonchiral cyanine dye and an enantiomeric lysine-derived amphiphile assembly shows circularly polarized luminescence with a high dissymmetry factor ($|g_{lum}| = 0.14$) in combination with strong emission (quantum yield $\phi = 0.70$, absorption coefficient $\varepsilon = 3.7 \times 10^5 \ M^{-1} \ cm^{-1}$). The circular polarization luminosity of the main transition band was calculated as 4.9×10^{-2}.

ROYAL SOCIETY OF CHEMISTRY

rsc.li/materials-advances

ROYAL SOCIETY
OF CHEMISTRY

COMMUNICATION

Check for updates

Co-assembling system that exhibits bright circularly polarized luminescence†

Naoya Ryu, [ID] *[a] Tomoyuki Harada,[b] Yutaka Okazaki, [ID] [c] Kyohei Yoshida, [ID] [a] Tomohiro Shirosaki, [ID] [a] Reiko Oda, [ID] [d] Yutaka Kuwahara, [ID] [b] Makoto Takafuji, [ID] [b] Hirotaka Ihara [ID] [be] and Shoji Nagaoka [ID] *[ab]

We demonstrate that a co-assembling system comprising a nonchiral cyanine dye and an enantiomeric lysine-derived amphiphile assembly show circularly polarized luminescence with a high dissymmetry factor ($|g_{lum}|$ = 0.14) in combination with strong emission (quantum yield ϕ = 0.70, absorption coefficient ε = 3.7 × 10⁵ M⁻¹ cm⁻¹). The circular polarization luminosity of the main transition band was calculated as 4.9 × 10⁻².

Materials that show circularly polarized luminescence (CPL) have major potential for applications including display devices,[1] security systems,[2] optical storage[3] and biological probes.[2,4] Such applications would primarily require both high polarization purity and strong emission intensity, *i.e.*, a high luminescence dissymmetry factor ($|g_{lum}|$), high emission quantum yield (ϕ) and high absorption coefficient (ε). g_{lum} is the ratio of the difference between the intensities for left- and right-handed CPL to the total emission intensity, and is represented by the following equation based on its relationship with the magnetic (m) and electric (μ) dipole moments:

$$g_{lum} = 4|m||\mu|\cos\theta/(m^2 + \mu^2) \tag{1}$$

where θ denotes the angle between these two moments.[5] For emissive organic molecules, because m is very small when compared with μ, eqn (1) can be simplified as follows:

$$g_{lum} \approx 4|m|\cos\theta/|\mu| \tag{2}$$

[a] Materials Development Department, Kumamoto Industrial Research Institute, 3-11-38 Higashimachi, Higashi-ku, Kumamoto 862-0901, Japan. E-mail: n-ryu@kumamoto-iri.jp, nagaoka@kumamoto-iri.jp

[b] Department of Applied Chemistry and Biochemistry, Kumamoto University, 2-39-1 Kurokami, Chuo-ku, Kumamoto 860-8555, Japan

[c] Graduate School of Energy Science, Kyoto University, Yoshida-Honmachi, Sakyo-ku, Kyoto 606-8501, Japan

[d] Institut de Chimie & Biologie des Membranes & des Nano-objets (UMR5248 CBMN), Centre National de la Recherche Scientifique (CNRS), Université de Bordeaux, Institut Polytechnique Bordeaux, 2 Rue Robert Escarpit, 33607 Pessac, France

[e] National Institute of Technology, Okinawa College, 905 Henoko, Nago, Okinawa 905-2192, Japan

† Electronic supplementary information (ESI) available: Experimental details and supplementary figures. See DOI: 10.1039/d2ma00002d

When the electric dipole transition is suppressed and the magnetic transition is allowed, $|g_{lum}|$ is higher. Conversely, both ϕ and ε are low in this case. It is thus generally difficult to achieve high $|g_{lum}|$ together with high ϕ and ε.

Some lanthanide complexes with chiral ligands have shown several emission peaks, and one or more of these peaks exhibited CPL with high $|g_{lum}|$.[1b,4b,6] For example, a europium complex with heptafluorobutyryl camphorate ligands showed high $|g_{lum}|$ within the region of one emission band from several bands.[6c] This CPL originated from the $^5D_0 \rightarrow {}^7F_1$ transition of europium(III), which is a magnetically allowed transition. Therefore, this CPL band's emission intensity is extremely low. Metal-free luminophores have also been investigated as CPL materials. Some of these materials showed strong emission with a single CPL band,[5,7] which may be advantageous when compared with lanthanide complex systems for practical applications. However, in almost all cases, $|g_{lum}|$ was below 10^{-2}.[5,7] There have been only a few reports of CPL luminophores with high $|g_{lum}|$ (>0.1) and ϕ (>0.5), which were cylindrical tetrameric luminophores[8] or solid film systems.[9] Although ε is an essential factor for efficient performance CPL systems as well as $|g_{lum}|$ and ϕ, the ε value was not discussed in these works.

Ihara *et al.* showed that a small nonchiral organic dye exhibited CPL with $|g_{lum}|$ of 0.10 when embedded in a self-assembly of glutamic acid-derived amphiphiles.[10] However, the dye's ϕ was not high (ϕ = 0.075). Additionally, Hachisako *et al.* reported that small organic dyes show intense emission when embedded in assemblies of appropriately designed amphiphiles derived from α-amino acids,[11] although their chiroptical properties were not evaluated. These findings indicate that a co-assembling system composed of small luminophores and chiral molecular assemblies represents a promising candidate to overcome the trade-off between g_{lum} and emission intensity.

In this communication, we show that CPL with a high $|g_{lum}|$ and strong emission is possible when using a co-assembling system comprising a nonchiral dye and a chiral template. As the chiral template, we used the assembly of an enantiomeric
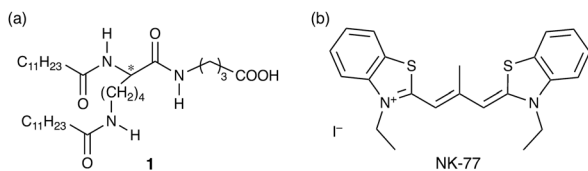
Fig. 1 Chemical structures of (a) lysine-derived amphiphile and (b) cyanine dye used in this study.

lysine-derived amphiphile with a double long alkyl chain **1** (see Fig. 1a). Some researchers have reported that chiral assemblies of glutamic acid-derived amphiphiles with a double long alkyl chain induce the chiral arrangement in nonchiral dyes,[10,12] while lysine-derived amphiphiles with that have not been used as the chiral templates so far. Because the side chain length of the amino acid residues of such amphiphiles should affect the morphology of the assemblies and the arrangement of the amphiphile molecules, it is important to investigate and understand the nature of assemblies of amphiphiles derived from lysine with a longer side chain in the field of chiral materials. The newly designed amphiphile **1** induced left- and right-handed CPL with a sharp band with $|g_{lum}| = 0.14$ in the nonchiral cyanine dye NK-77 (Fig. 1b). The ϕ and ε values of NK-77 were enhanced by the co-assembling process to be 0.70 and 3.7×10^5 M^{-1} cm^{-1}, respectively. Furthermore, we calculated circular polarization luminosity (Λ_{CPL}) based on the main 0–0 bands,[13] which represents CPL efficiency in consideration of ϕ and ε in addition to g_{lum}, to be 4.9×10^{-2} according to the following equation:

$$\Lambda_{CPL} = f \times \phi \times (|g_{lum}|/2) \tag{3}$$

where f denotes the oscillator strength for absorbance.[5]

Amphiphile **1** was newly synthesized using a previously reported procedure (see ESI,† Scheme S1 and Fig. S1–S3).[11]

Amphiphile **1** could be dissolved in water at pH 10 or more by heating, while it could not be completely dissolved below pH 9. This suggests that the acid dissociation constant (pK_a) of the carboxylic acid of **1** increases by the aggregation effect compared to molecularly dispersed carboxylic acid compounds such as acetic acid (pK_a = 4.7).[14] Taking into account the possibility of the hydrolysis of **1** with amide bonds in too high pH conditions, the pH was set to 10 in this work.

Scanning transmission electron microscopy (STEM) and scanning electron microscopy (SEM) showed that **1** spontaneously formed flat- or rolled-ribbon-like assemblies with varying width and pitch in water at pH 10 and 20 °C (Fig. 2b, inset (upper left), and Fig. S4, ESI†). Rolled ribbons of L-**1** were exclusively right-handed, while those of D-**1** were left-handed. These assemblies showed an endothermic peak at 64 °C (enthalpy ΔH = 62 kJ mol^{-1}) in a differential scanning calorimetry (DSC) curve during the heating process, as shown in Fig. 2a. This peak is ascribed to the gel-to-liquid crystalline phase transition temperature (T_c), thus indicating that the assembly of **1** is based on a bilayer structure. Note that inorganic salts can affect the morphology and T_c of ionic amphiphile assemblies.[11] When NaCl was added to the **1**
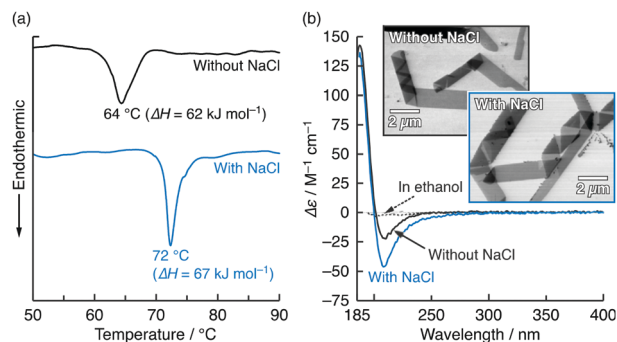

Fig. 2 (a) DSC thermogram of heating process for L-**1** (5 mM) in basic water without and with NaCl (250 mM); heating rate: 2 °C min^{-1}. (b) CD spectra of L-**1** (0.2 mM) in water at pH 10 without and with NaCl (10 mM) and in ethanol at 20 °C. Insets in (b) show STEM images of L-**1** assemblies in cast films prepared from 0.2 mM aqueous dispersions without and with NaCl (10 mM) at pH 10 when post-stained with OsO₄. UV absorption spectra corresponding to (b) are shown in Fig. S6 (ESI†).

aqueous dispersion ([**1**]:[NaCl] = 1 : 50 mol/mol), T_c and ΔH increased to 72 °C and 67 kJ mol^{-1} (Fig. 2a), respectively, although no visible assembly shape modification was observed (Fig. 2b, inset (lower right), and Fig. S5, ESI†). Fig. 2b shows the circular dichroism (CD) spectra of L-**1** in basic water (pH 10) with and without NaCl, along with that in ethanol, which is a good solvent for **1**. In water without NaCl, the CD signal was detected in the ultraviolet (UV) absorption region ascribed to the amide bonds and carboxylate of L-**1** (Fig. S6, ESI†). No CD signal was observed for L-**1** in ethanol (Fig. 2a). These results indicate that the CD signal for L-**1** in water is due to the chirally arranged secondary structure in the assembly. The chiral interaction between the L-**1** molecules was clearly affected by NaCl. As NaCl was added to the L-**1** aqueous dispersion ([**1**]:[NaCl] = 1 : 50 mol/mol), the CD signal increased obviously. The increases in T_c, ΔH and the CD signal indicate that in the presence of NaCl, the **1** molecules interact with each other more strongly and are probably arranged more chirally because of the screening of the electrostatic repulsion between the adjacent carboxylates caused by the charge neutralization and the dehydration by Na⁺.

Chiral amphiphile assemblies can induce CD in nonchiral small dyes when they are co-assembled.[10,12,15] Fig. 3 shows the visible absorption and CD spectra of the cationic cyanine dye NK-77 (0.01 mM) in the presence of the assembled amphiphile L-**1** (0.2 mM) in water at pH 10 containing various NaCl concentrations (0–50 mM) at 20 °C. Although NK-77 alone is too hydrophobic to be water-soluble, it could be dissolved in water at pH 10 with the support of the **1** assembly. Cationic NK-77 should bind electrostatically to the anionic **1** assembly and be co-assembled. In the presence of L-**1**, NK-77 showed a bisignate CD signal in the absorption band region with peaks at 577 (negative) and 565 nm (positive). Because NK-77 is nonchiral, this CD signal is due to the chirality induced by the chiral assembly of L-**1**. The CD signal's bisignate shape indicates that the induced CD was mainly caused by exciton coupling among the NK-77 molecules.[16] The ellipticity was
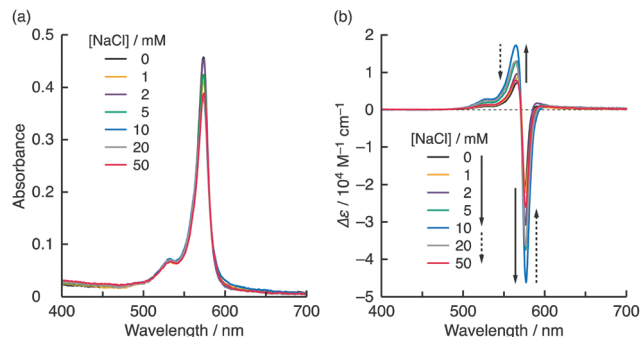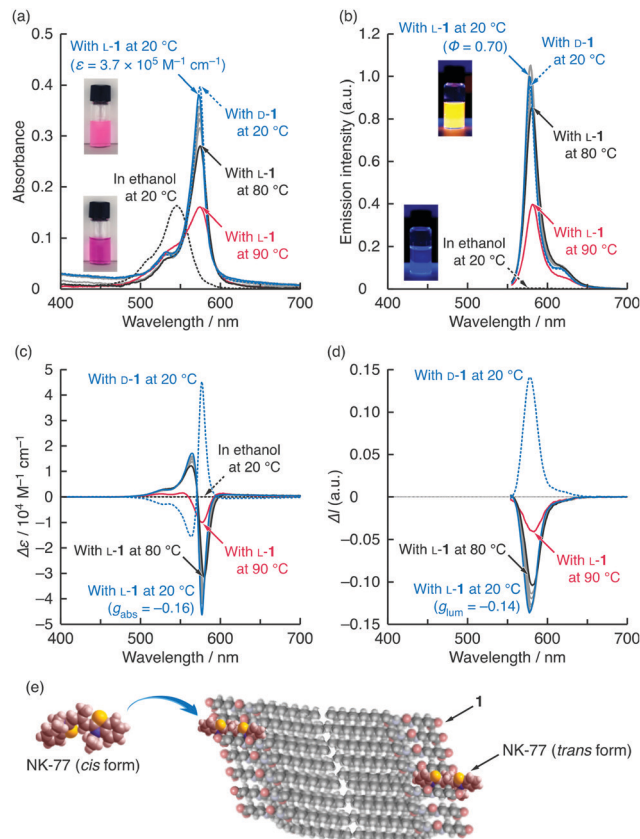
Fig. 3 (a) Visible absorption and (b) CD spectra of NK-77 (0.01 mM) in the presence of L-**1** (0.2 mM) in water at pH 10 containing various NaCl concentrations at 20 °C; path length: 0.1 cm. Variations in absorbance and $\Delta\varepsilon$ as functions of NaCl concentration are shown in Fig. S7 (ESI†).

sensitive to the NaCl concentration, but the absorption spectra did not change significantly. When the NaCl concentration was increased, the CD signal gradually increased in tandem, reaching a maximum at 10 mM ([L-**1**]:[NaCl] = 1 : 50 mol/mol) (Fig. 3 and Fig. S7, ESI†). This CD signal enhancement is probably caused by the enhancement in the chiral arrangement of the L-**1** molecules, which is due to relaxation of the electrostatic repulsion between the carboxylates caused by Na$^+$. The maximum absorbance dissymmetry factor ($|g_{abs}|$) was calculated to be 0.16 at 579 nm (Fig. S8a, ESI†). To the best of our knowledge, such an extremely high $|g_{abs}|$ has not been achieved previously *via* exciton coupling among the chromophores alone. Therefore, it may be reasonable to conclude that the cause of the CD induced in the present co-assembling system also contains an asymmetric perturbation of the NK-77 caused by the chiral **1** assembly and/or coupling of the electric transition moments between **1** and NK-77.[16] Further increases in the NaCl concentration led to reduction of the ellipticity (Fig. 3 and Fig. S7, ESI†), indicating that excess NaCl disturbed the chiral arrangement of the **1** molecules. At concentrations exceeding 100 mM, the co-assembly was precipitated, in a manner similar to salting out.

Fig. 4a–d shows the visible absorption, emission, CD and CPL spectra of NK-77 (0.01 mM) in the presence of the assembled amphiphiles L-**1** and D-**1** (0.2 mM) in NaCl aqueous solutions (10 mM) at pH 10 and alone in ethanol at various temperatures. The molar ratios of NK-77 : **1** : NaCl were set at 1 : 20 : 1000, at which the CD signal and g_{abs} reached their highest values (Fig. 3 and Fig. S10, ESI†). NK-77 showed mirror image CD signals in the presence of the L-**1** and D-**1** assemblies (Fig. 4c). The CD signal directions indicate that the NK-77 molecules form an S-chiral (left-handed) arrangement in the L-**1** assembly and an R-chiral (right-handed) arrangement in the D-**1** assembly.[17] At this molar ratio, their flat or rolled-ribbon-like nanostructures were maintained (Fig. S11, ESI†), and T_c remained almost constant (Fig. S12, ESI†) with or without NK-77. As shown in Fig. 4b and d, NK-77 co-assembled with L-**1** and D-**1** showed both strong emission and large mirror-image CPL signals. For NK-77 in the presence of the L-**1** assembly at 20 °C, ϕ was estimated to be 0.70, and the maximum $|g_{lum}|$ reached

Fig. 4 (a) Visible absorption, (b) emission, (c) CD and (d) CPL spectra of NK-77 (0.01 mM) in the presence of L-**1** and D-**1** (0.2 mM) in water at pH 10 containing NaCl (10 mM) and alone in ethanol measured at different temperatures (20–90 °C); path length: 0.1 cm (for (a)); excitation wavelengths: 545 (for (b)) and 510 nm (for (d)). Insets show images of the NK-77–L-**1** aqueous mixture containing NaCl and NK-77 ethanol solution at room temperature in (a) daylight and (b) under 365 nm UV light in the dark. Variations in absorbance, emission intensity, $\Delta\varepsilon$ and ΔI as a function of temperature are shown in Fig. S9 (ESI†). (e) Schematic illustration of simulated model of NK-77 dispersed in polar solvent (*cis* form) and embedded in **1** assembly (*trans* form).

0.14 at 586 nm (Fig. S8b, ESI†). This $|g_{lum}|$ value is the highest reported for low-molecular-weight metal-free dyes in dilute solutions or dispersion systems.

When compared with molecularly dispersed NK-77 in ethanol at 20 °C, which has an absorption peak at 545 nm (0–0 band) with a shoulder around 505 nm (0–1 band),[13] NK-77 in the presence of L-**1** had a larger, red-shifted absorption peak at 574 nm (Fig. 4a). In addition, NK-77 in the presence of L-**1** showed enhanced emission at 579 nm with a small Stokes shift of 150 cm^{-1} (5 nm) (Fig. 4b). At first glance, the red-shifted absorption peak and the strong emission appear to be caused by J-aggregation. However, for the following reasons, we ascribed these peaks to the monomeric species that are electrostatically bound to L-**1** and embedded in the hydrophobic cavities of the L-**1** assembly by the hydrophobic effect, as illustrated in Fig. 4e. When the NK-77–L-**1** dispersion was heated, no additional peak was observed at 545 nm at the same time as the reduction in the peak at 574 nm (Fig. 4a).

Furthermore, the NK-77–L-**1** composite had an emission lifetime of 1.7 ns (Fig. S13, ESI†). These behaviours differ from those of typical J-aggregates of cyanine dyes. J-aggregated species of cyanine dyes are easily dissociated into monomeric species by heating[18] and have short emission lifetimes on the picosecond time scale.[19] These behaviours indicate that the red shift in the absorption peak mainly results from formation of the *trans* isomer of NK-77 in the hydrophobic microenvironment of the **1** assembly (Fig. 4e).[20] Therefore, we conclude that exciton coupling occurred among the embedded NK-77 molecules without direct stacking, but with a distance between them. Embedding NK-77 in the tightly packed cavity is accompanied by restriction of the internal rotations, including photoisomerization to the *cis* form. NK-77, which have a *meso*-methyl substituent, in polar ethanol should form the *cis* isomer with a higher intramolecular degree of freedom.[20] Restriction of the internal rotation of the embedded NK-77 molecules also resulted in increases in both absorbance and emission. The absorbance was 2.5 times higher than that of NK-77 in ethanol (Fig. 4a). The ε value was estimated to be 3.7×10^5 M^{-1} cm^{-1} at 20 °C. The main emission peak was remarkably sharp, with a full width at half maximum of 480 cm^{-1} (16 nm), which was more than 100 times higher than that of NK-77 in ethanol (Fig. 4b).

From the obtained spectra of the NK-77–L-**1** composite at 20 °C, we calculated Λ_{CPL} of the main 0–0 band after peak separation (Fig. S14, ESI†). In the case of the Λ_{CPL} calculation, f is used as the factor of absorption efficiency instead of ε, and is determined through absorption spectra using the following equation:

$$f = 4.32 \times 10^{-9} \int \varepsilon(\tilde{v}) d\tilde{v} \qquad (4)$$

where $\tilde{v}$ denotes the wavenumber in cm^{-1}.[21] According to eqn (4), f of the main band was calculated as 1.1. ϕ of the main band was estimated from the ratio between the integrated area of 0–0 and 0–1 emission bands to be 0.60. $|g_{lum}|$ was calculated from the emission and CPL spectra of the main bands to be 0.15. From these values, we determined Λ_{CPL} of the main 0–0 band as 4.9×10^{-2} using eqn (3).

Embedding of NK-77 in the **1** assembly also contributed to preventing its colour from fading. It is well-known that cyanine dyes are easily degraded by both oxygen and light.[22] Indeed, the absorbance of NK-77 in undegassed ethanol decreased by 74% after 1 month from initial preparation (Fig. S15, ESI†), despite being stored in the dark at 20 °C. In contrast, no such reduced absorbance was observed for NK-77 embedded in the L-**1** assembly in undegassed water stored under the same conditions (Fig. S15, ESI†), which indicates that NK-77 molecules embedded in the L-**1** assembly are protected from molecular oxygen dissolved in the water.

It was noted that chiroptical signals are strongly affected by the linear dichroism (LD) component. Therefore, we measured LD and CD spectra of the NK-77–L-**1** co-assembly at 20 °C using the same spectropolarimeter and then investigated the effect of LD on the CD signals. The NK-77–L-**1** co-assembly showed an
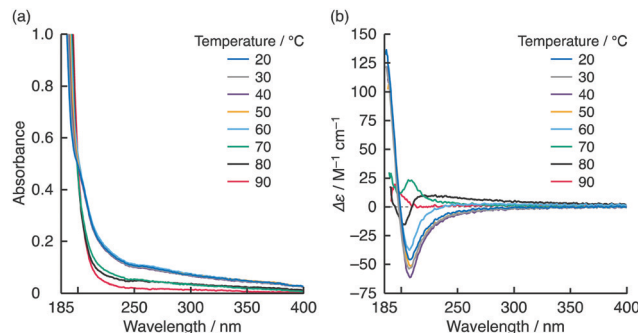

Fig. 5 (a) UV absorption and (b) CD spectra of L-**1** (0.2 mM) in water at pH 10 containing NaCl (10 mM) measured at various temperatures (20–90 °C); path length: 0.1 cm. Variations in absorbance at 300 nm and $\Delta\varepsilon$ at 208 nm as a function of temperature are shown in Fig. S16 (ESI†).

LD signal in the region of the absorption and CD bands. The LD signal intensity changed dramatically at every shaking of the co-assembly dispersion, while the CD signal did not change (Fig. S16, ESI†). These results indicate that the LD contribution to the chiroptical signals of the NK-77–**1** co-assembly is negligible.

The optical spectra of the NK-77–L-**1** co-assembly were almost entirely resistant to heat up to 80 °C (Fig. 4 and Fig. S9, ESI†). The $|g_{abs}|$ and $|g_{lum}|$ values at 80 °C were both estimated to be 0.15. This temperature is higher than the T_c of the L-**1** assembly containing NaCl and NK-77 (Fig. S12, ESI†). Over 80 °C, the optical peaks and signals were reduced drastically (Fig. 4 and Fig. S9, ESI†). During the heating process, the CD signal of the L-**1** assembly itself changed dramatically and its turbidity decreased at 70 °C (Fig. 5 and Fig. S17, ESI†), which corresponds to the gel-to-liquid crystalline phase transition. In the 70–90 °C range, the CD signal changed intricately, although it did not disappear (Fig. 5b and Fig. S17b, ESI†). This indicates that although the molecular arrangements of **1** are different in the ranges between 20–60 °C and 70–90 °C, the **1** molecules are arranged chirally even above T_c. Additionally, the **1** aqueous dispersion remained visually turbid, even when it was heated to 70–80 °C, and it became clear at 90 °C, as confirmed from the UV absorption spectra (Fig. 5a and Fig. S17a, ESI†). This sudden change in turbidity indicates that the aggregation morphology of the **1** molecules changed further at 90 °C. We therefore deduce that this morphological change contributes to the reductions in the optical peaks and signals for NK-77 in the presence of the L-**1** assembly at 90 °C.

Conclusions

In conclusion, CPL with both high $|g_{lum}|$ and strong emission was induced in a small metal-free dye by embedding it in an enantiomeric lysine-derived amphiphile assembly. The present CPL system had Λ_{CPL} of 4.9×10^{-2}. Although almost all papers on CPL systems have not calculated Λ_{CPL}, we believe that this value is extremely large compared to the most of previously reported CPL systems. The key to attaining such high $|g_{lum}|$ in combination with high ϕ and ε is that the dye molecules are

packed tightly and are arranged chirally without direct stacking in the hydrophobic chiral microenvironment. This co-assembling route offers a versatile and efficient method to design systems with strong chiroptical signals that are highly emissive while avoiding the complexity of molecular design and synthesis of chiral luminophores. Furthermore, the chiral foundation is derived from α-amino acids, which is advantageous for many practical applications because α-amino acid enantiomers are commercially available and opposing CPL signals can be obtained easily.

The findings presented here will not only lead to improved understanding of the chiroptical behaviour of small molecules interacting with molecular assemblies, but also will provide a new strategy for optically active luminescent materials design.

Author contributions

N. Ryu designed the study, raised a fund, performed almost all the experiments, and wrote the manuscript with assistance from all other authors. T. Harada confirmed the chemical structure of the amphiphile. Y. Okazaki assisted with design of the study, raised funds, and measured some of the CPL spectra. K. Yoshida measured the emission lifetimes. T. Shirosaki and S. Nagaoka assisted with the molecular simulations. R. Oda raised a fund and assisted with the CPL spectral measurements. Y. Kuwahara also assisted with the CPL spectral measurements. M. Takafuji and H. Ihara assisted with confirmation of the chemical structure of the amphiphile and the emission spectral measurements. All authors discussed the results and contributed to the interpretation of the data.

Conflicts of interest

There are no conflicts to declare.

Acknowledgements

Notes and references

1 (a) Y. Yang, R. C. Da Costa, D. M. Smilgies, A. J. Campbell and M. J. Fuchter, *Adv. Mater.*, 2013, **25**, 2624; (b) F. Zinna, M. Pasini, F. Galeotti, C. Botta, L. Di Bari and U. Giovanella, *Adv. Funct. Mater.*, 2017, **25**, 1603719.

2 J. W. Grate and G. C. Frye in *Sensors Update*, ed. H. Baltes, W. Göpel and J. Hesse, Wiley-VCH, Weinheim, 1996, Vol. 2, 10–20.

3 C. Wagenknecht, C.-M. Li, A. Reingruber, X.-H. Bao, A. Goebel, Y.-A. Chen, Q. Zhang, K. Chen and J.-W. Pan, *Nat. Photonics*, 2010, **4**, 549.

4 (a) G. Muller, *Dalton Trans.*, 2009, 9692; (b) F. Zinna and L. Di Bari, *Chirality*, 2015, **27**, 1.

5 T. Mori, *Chem. Rev.*, 2021, **121**, 2373.

6 (a) J. P. Leonard, P. Jensen, T. McCabe, J. E. O'Brien, R. D. Peacock, P. E. Kruger and T. Gunnlaugsson, *J. Am. Chem. Soc.*, 2007, **129**, 10986; (b) Y. Hasegawa, *Bull. Chem. Soc. Jpn.*, 2014, **87**, 1029; (c) J. Kumar, B. Marydasan, T. Nakashima, T. Kawai and J. Yuasa, *Chem. Commun.*, 2016, **52**, 9885.

7 (a) J. Kumar, T. Nakashima, H. Tsumatori, M. Mori, M. Naito and T. Kawai, *Chem. – Eur. J.*, 2013, **19**, 14090; (b) Y. Sasai, R. Inoue and Y. Morisaki, *Bull. Chem. Soc. Jpn.*, 2020, **93**, 1193; (c) H. Kubo, T. Hirose, D. Shimizu and K. Matsuda, *Chem. Lett.*, 2021, **50**, 804.

8 S. Sato, A. Yoshii, S. Takahashi, S. Furumi, M. Takeuchi and H. Isobe, *Proc. Natl. Acad. Sci. U. S. A.*, 2017, **114**, 13097.

9 (a) J. Liu, H. Su, L. Meng, Y. Zhao, C. Deng, J. C. Y. Ng, P. Lu, M. Faisal, J. W. Y. Lam, X. Huang, H. Wu, K. S. Wong and B. Z. Tang, *Chem. Sci.*, 2012, **3**, 2737; (b) J. Wade, J. R. Brandt, D. Reger, F. Zinna, K. Y. Amsharov, N. Jux, D. L. Andrews and M. J. Fuchter, *Angew. Chem., Int. Ed.*, 2021, **60**, 222.

10 T. Goto, Y. Okazaki, M. Ueki, Y. Kuwahara, M. Takafuji, R. Oda and H. Ihara, *Angew. Chem., Int. Ed.*, 2017, **56**, 2989.

11 H. Hachisako, N. Ryu and R. Murakami, *Org. Biomol. Chem.*, 2009, **7**, 2327.

12 (a) H. Matsukizono, K. Kuroiwa and N. Kimizuka, *J. Am. Chem. Soc.*, 2008, **130**, 5622; (b) D. Yang, C. Liu, L. Zhang and M. Liu, *Chem. Commun.*, 2014, **50**, 12688.

13 W. West and S. Pearce, *J. Phys. Chem.*, 1965, **69**, 1894.

14 J. R. Kanicky, A. F. Poniatowski, N. R. Mehta and D. O. Shah, *Langmuir*, 2000, **16**, 172.

15 (a) N. Ryu, Y. Okazaki, K. Hirai, M. Takafuji, S. Nagaoka, E. Pouget, H. Ihara and R. Oda, *Chem. Commun.*, 2016, **52**, 5800; (b) N. Ryu, Y. Okazaki, E. Pouget, M. Takafuji, S. Nagaoka, H. Ihara and R. Oda, *Chem. Commun.*, 2017, **53**, 8870.

16 S. Allenmark, *Chirality*, 2003, **15**, 409.

17 N. Berova and K. Nakanishi, in *Circular Dichroism: Principles and Applications*, ed. N. Berova, K. Nakanishi and R. Woody, Wiley-VCH, New York, 2nd edn, 2000, Ch. 12.

18 T. Harada, M. Kurihara, R. Kuroda and H. Moriyama, *Chem. Lett.*, 2012, **41**, 1442.

19 J. L. Bricks, Y. L. Slominskii, I. D. Panas and A. P. Demchenko, *Methods Appl. Fluoresc.*, 2018, **6**, 012001.

20 P. Pronkin and A. Tatikolov, *Sci*, 2019, **1**, 19.

21 A. Belay, *Food Chem.*, 2010, **121**, 585.

22 N. S. James, R. R. Cheruku, J. R. Missert, U. Sunar and R. K. Pandey, *Molecules*, 2018, **23**, 1842.